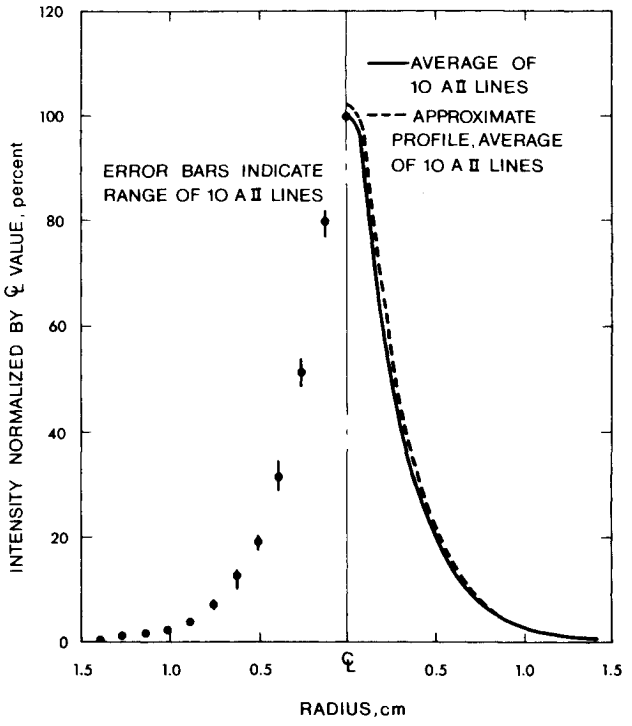

Fig. 4 Arc region intensity, normalized by centerline value, as a function of radial position.

modified slightly to provide improved cathode spot stability. All data were taken with an argon mass flow rate of 0.1 g/sec, background tank pressure of 7.5×10^{-2} torr, current of 125 amp at 20 v and zero applied magnetic field. A 0.5-m scanning monochromator with photomultiplier detector, front surface mirrors and achromatic lenses were used as shown in Fig. 1 to measure intensity integrated along the axial direction as a function of radial position. In addition, lateral intensities, integrated over the plume diameter, were measured at six stations downstream from the accelerator exit plane. The optical response of the system was calibrated before and after each run by replacing the source with a tungsten standard lamp.

Preliminary spectra were taken to aid in the choice of the representative spectral lines shown in Table 1. Ten AII lines, nine AI lines, and ten continuum values were chosen on the bases of representative strength, freedom from interference from other lines, freedom from self-absorption,[10-13] and positive source identification.

Results and Discussion

Results indicating the range of intensities measured in the plume are shown in Fig. 2, while profiles of absolute intensity normalized by the corresponding arc region value are shown in Fig. 3. Comparison of these two figures indicates that AII radiation dominates the arc region. Since the distribution of normalized AII plume intensity, shown in Fig. 3, exhibits so little scatter, it can be redefined in terms of the arc intensity which was used for normalization. This allows a simplification of Eq. (1) for the AII species, such that

$$I_{\text{arc}} = \frac{4\pi L \Delta\lambda}{S_{\text{cal}}} \frac{(S - S_{\text{cath}})}{(I_{\text{arc}} + F)} \tag{2}$$

where F is the integral of the normalized AII intensity distribution along the line of sight. This form makes it easy to visualize the error introduced by neglecting the radiation from the exhaust plume ($I_{\text{arc}} + F \simeq I_{\text{arc}}$) and the cathode ($S - S_{\text{cath}} \simeq S$).

An example of this error is indicated in Fig. 4, where a radial profile of AII arc intensity, normalized by the corresponding centerline value is shown, along with the approximate intensity profile obtained by neglecting the plume and cathode contributions in Eq. (2). The error introduced by this approximation ranges from 1.1% to 2.1% of the corrected value and is consistent for all AII lines measured.

For this typical plasma accelerator, the AII species dominates the arc region, and the AII intensity in the arc region is substantially higher than that of the exhaust plume or the corresponding continuum radiation from the cathode. Thus, the AII arc region intensity may be closely approximated by neglecting the plume and continuum contributions.

References

[1] Connolly, D. J. et al., "Low Environmental Pressure MPD Arc Tests," *AIAA Journal*, Vol. 6, No. 7, July 1968, pp. 1271–1276.

[2] Bohn, W. L., Beth, M.-U., and Nedder, G., "On Spectroscopic Measurements of Velocity Profiles and Non-Equilibrium Radial Temperatures in an Argon Plasma Jet," *Journal of Quantitative Spectroscopy and Radiative Transfer*, Vol. 7, 1967, pp. 661–676.

[3] Adcock, B. D., "Temperature Measurements on a Subatmospheric Argon Plasma Jet," *Journal of Quantitative Spectroscopy and Radiative Transfer*, Vol. 7, 1967, pp. 385–400.

[4] Freeman, M. P., "A Quantitative Examination of the LTE Condition in the Effluent of an Atmospheric Pressure Argon Plasma Jet," *Journal of Quantitative Spectroscopy and Radiative Transfer*, Vol. 8, 1968, pp. 435–450.

[5] Sovie, R. J. and Connolly, D. J., "A Study of the Axial Velocities in an Ammonia MPD Thruster," *AIAA Journal*, Vol. 7, No. 4, April 1969, pp. 723–725.

[6] Knopp, C. F., Gottschlich, C. F., and Cambel, A. B., "The Spectroscopic Measurement of Temperature in Transparent Argon Plasmas," *Journal of Quantitative Spectroscopy and Radiative Transfer*, Vol. 2, 1962, pp. 297–299.

[7] Grossman, W., Jr., "Theory and Experiment of a Coaxial Plasma Accelerator," Ph.D. thesis, 1964, Virginia Polytechnic Institute and State Univ., Blacksburg, Va., pp. 34–39.

[8] Larson, A. V., "Experiments on Current Rotations in an MPD Engine," *AIAA Journal*, Vol. 6, No. 6, June 1968, pp. 1001–1006.

[9] Shih, K. T., "Anode Current and Heat Flux Distribution in an MPD Engine," *AIAA Journal*, Vol. 8, No. 2, Feb. 1970, pp. 377–378.

[10] Olsen, H. N., "The Electric Arc as a Light Source for Quantitative Spectroscopy," *Journal of Quantitative Spectroscopy and Radiative Transfer*, Vol. 3, 1963, pp. 305–333.

[11] Malone, B. S. and Corcoran, W. H., "Transition Probability Measurements in the Blue-Near-U.V. Spectrum of Argon I," *Journal of Quantitative Spectroscopy and Radiative Transfer*, Vol. 6, 1966, pp. 443–449.

[12] Tourin, R. H., "Optically Thick Plasmas," *Journal of Quantitative Spectroscopy and Radiative Transfer*, Vol. 3, 1963, pp. 89–90.

[13] Tidwell, E. D., "Transition Probabilities of Argon II," *Journal of Quantitative Spectroscopy and Radiative Transfer*, Vol. 12, 1972, pp. 431–441.

On the Structure of Jet Plumes

JOHN H. FOX*
ARO, Inc., Arnold Air Force Station, Tenn.

Nomenclature

d_j = diameter of nozzle at exit plane
l = axial distance from nozzle exit to Mach disk
M_E = exit Mach number of nozzle
p_E = static pressure at nozzle exit
p_∞ = ambient pressure
S = diameter of Mach disk
x_b = axial distance from nozzle exit to body (Fig. 5)
γ = ratio of specific heats
θ_N = half-angle of nozzle exit
ω = axial distance from nozzle exit to intersection of reflected shock with plume boundary (primary wavelength)

Received June 15, 1973; revision received August 30, 1973.
Index category: Jets, Wakes, and Viscid-Inviscid Flow Interactions.
* Scientific Programmer.

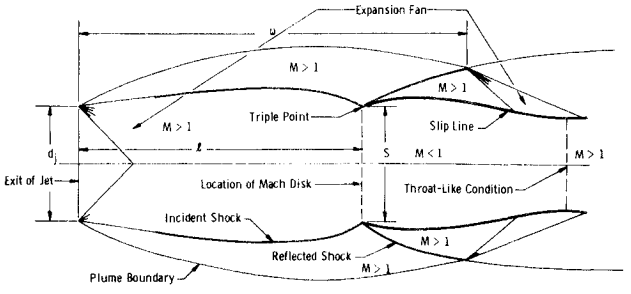

Fig. 1 Computational schematic of typical exhaust plume.

Introduction

ABBETT[1] proposed a criterion for locating the Mach disk in underexpanded supersonic exhaust plumes. Utilizing this criterion in a method of characteristics computer program, he was able to show good agreement with data from Love et al.[2] for one nozzle exit condition. It is the purpose of this Note to present the results obtained from the application of the Abbett theory to other nozzle exit conditions and to compare them with the Love data and with three data points provided by Peters.[3] The comparisons demonstrate that the method of characteristics coupled with the Abbett criterion is quite good as a theoretical tool for the detailed analysis of the structure of jet plumes exhausting into still air. It enables one to predict the position of the Mach disk, the primary wavelength, and the position of the throat-like constriction where the subsonic flow downstream of the Mach disk reaccelerates to the supersonic condition.

Theory

With reference to Fig. 1, the theory predicts that the triple point will be uniquely determined by the requirement that the quasi-one-dimensional subsonic flow, at the downstream side of the Mach disk, accelerate smoothly through a throatlike critical region formed by the slipline between the subsonic core and the outer, completely supersonic flow.

The preceding criterion was introduced in a straightforward way into an existing method of characteristics program,[4] the details of which will not be presented here. It will be noted only that the differences between this program and that of Abbett are: in the present program, the shock slopes are averaged to obtain the incident and reflected shock point locations, the streamline properties are determined as required by interpolation within the mesh, and the procedure for locating the Mach disk is set up

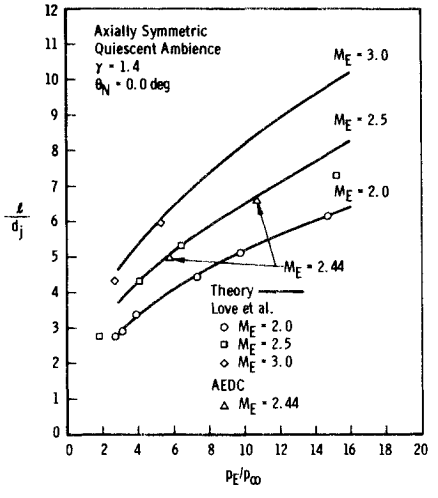

Fig. 2 Position of Mach disk vs static pressure ratio.

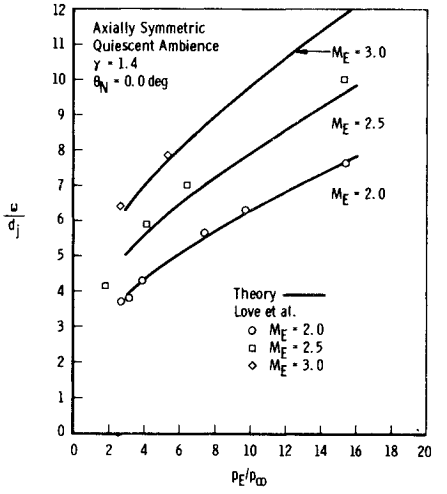

Fig. 3 Primary wavelength vs static pressure ratio.

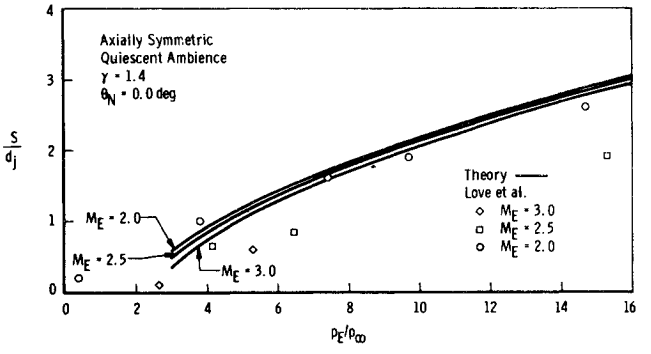

Fig. 4 Mach disk diameter vs static pressure ratio.

in the form of an iteration using the halving technique. The upstream bound is taken to be that Mach disk location where the quasi-one-dimensional core remains subsonic through the constriction. The downstream bound is taken as that location where the converging slipline decreases in radius below the critical throat radius as determined by one-dimensional gas-dynamics.

As it was not of interest to actually pass through the throat-like region, the computation was terminated when the updated guess of the axial distance to the Mach disk changed less than 0.05% of the last guess.

Comparison with Experiments

The work of Love is generally well known, readily available, and needs no elaboration. It is presented in Figs. 2–4 along with the corresponding theoretical curves. The comparisons illustrate the quality of the predictions. Except for the Mach disk diameters, the correlation is good. The reasons for the poor correlation between Mach disk diameters are not obvious.

The work of C. E. Peters and R. A. Paulk at the Engine

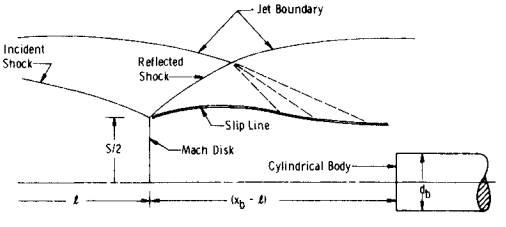

Fig. 5 Schematic of AEDC experiment.

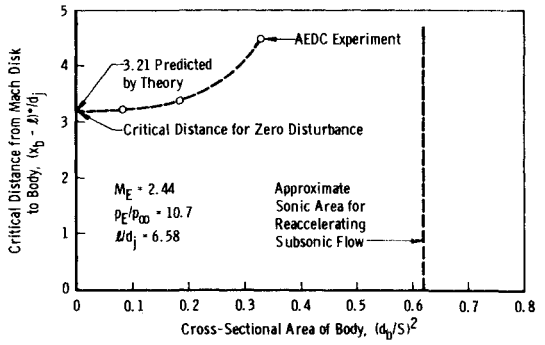

Fig. 6 Position of critical station downstream of Mach disk.[3]

Test Facility of the AEDC offers three additional data points for comparison, two of which were obtained with a Mach 2.44 nozzle and are presented in Fig. 2. At a p_E/p_∞ of 5.75, an l/d_j of 4.96 was obtained as against the theoretical prediction of 4.94. Again at a p_E/p_∞ of 10.7, an l/d_j of 6.58 was recorded compared with the prediction of 6.53.

A third experiment was devised by Peters to determine the location of the sonic region. In that experiment, shown schematically in Fig. 5, blunt cylindrical bodies of various diameters were translated upstream towards the Mach disk of the Mach 2.44 nozzle. At some critical body position, $(x_b - l)^*$, observation with shadowgraph showed the location of the Mach disk to be affected by the particular body. By extrapolation of the experimental critical distances to zero body diameter (i.e., to zero disturbance), the location of the critical station was established. The results presented in Fig. 6 for $p_E/p_\infty = 10.7$ show that the critical station is located approximately 3.2 nozzle diameters downstream of the Mach disk. The theory predicts a corresponding distance of 3.21 diameters. The extremely close correlation is of course fortuitous, but even accepting error in the experimental procedure, the agreement is quite good.

References

[1] Abbett, M., "The Mach Disk in Underexpanded Exhaust Plumes," *AIAA Journal*, Vol. 9, No. 3, March 1971, pp. 512–514.

[2] Love, E. S., Grigsby, C. E., Lee, L. P., and Woodling, M. J., "Experimental and Theoretical Studies of Axisymmetric Free Jets," TR R-6, 1959, NASA.

[3] Peters, C. E., private communication, Jan. 1973, Arnold Engineering Development Center, Arnold Air Force Station, Tenn.

[4] Fox, J. H., "Axially Symmetric, Inviscid, Real Gas, Non-isoenergetic Flow Solution by the Method of Characteristics," AEDC TR-69-184, Jan. 1970, Arnold Engineering Development Center, Arnold Air Force Station, Tenn.

Specific Heat of X14 Propellant

J. RICHARD WARD*
Ballistic Research Laboratories, Aberdeen Proving Ground, Md.

Nomenclature

$\bar{C}_p$ = specific heat of sample
$\bar{C}_{p_{std}}$ = specific heat of sapphire standard
m_s = mass of sample
m_{std} = mass of sapphire standard
ΔY_s = magnitude of thermal lag for sample
ΔY_{std} = magnitude of thermal lag for sapphire standard

Received June 25, 1973.

Index categories: Fuels and Propellants, Properties of; Liquid and Solid Thermophysical Properties; Thermal Surface Properties.

* Chemist, Combustion and Propulsion Branch, Interior Ballistics Lab.

Introduction

RESEARCH is in progress in our laboratory to measure and eventually model the temperature sensitivity of solid propellant combustion. Current experiments are being conducted with X14, a solid, nitroglycerin-nitrocellulose double-base propellant. The specific heat of the condensed phase is one physical parameter needed to compare experiments with proposed models. In the past the specific heat was calculated by summing the atomic contributions to the heat capacity, and then dividing by the propellant's molecular weight. Measured heat capacities are not available for NC-NG double-base propellants; instead the calculated specific heat must be used over the temperature range of interest. Kirby and Suh[1] calculated the condensed phase contribution to the over-all heat of reaction of M2 propellant using a constant calculated value of 0.27 cal/g-°C for the specific heat of solid M2 over a 125°C range. For X14 propellant, not even a calculated specific heat is available, so it was decided to measure the specific heat with a differential scanning calorimeter. This will provide accurate specific heat data for the X14 temperature sensitivity experiments, as well as a measured specific heat to compare with the calculated specific heats for NC-NG double-base propellants. Since the differential scanning calorimeter measures specific heat continuously with changing temperature, the assumption that the propellant's specific is temperature invariant may be tested too.

Experimental

Specific heats were measured with a thermal analyzer (DuPont model 990) equipped with the differential scanning calorimeter (DSC) module. This DSC cell makes use of a constantan disk with two raised platforms for the aluminum sample and reference pans. The constantan disk serves as the primary means of heat transfer to the sample and reference pans. The thermal lag between these is proportional to the mass and specific heat of the sample and reference systems for a given heating rate. Specific heats are determined by comparing the thermal lag under "blank" and "sample" conditions. A blank run consists of two empty aluminum sample and reference pans; the sample was rerun under identical conditions with the X14 propellant added to the sample pan. Baxter[2] reports that specific heats of polymeric materials may be determined to within 5% of existing values with this type DSC cell. The DSC cell has a calorimetric sensitivity of 0.05 mcal/sec-in.

Three disks of X14 propellant were cut from the center of a block of the same propellant lot used in the temperature sensitivity experiments. Specific heats were measured from 10°C to 70°C, since a heating curve of weight vs temperature of X14 propellant obtained with a thermogravimetric analyzer

Table 1 Specific heat of X14 propellant samples[a]

Temp, °K	$\bar{C}_p$X14[b]	$\bar{C}_p$X14[c]	$\bar{C}_p$X14[d]
283	0.307	0.306	0.299
288	0.309	0.309	0.302
293	0.315	0.315	0.307
298	0.317	0.318	0.310
303	0.322	0.323	0.313
308	0.324	0.326	0.317
313	0.327	0.330	0.320
323	0.333	0.338	0.326
333	0.340	0.452	0.332
343	0.345	0.347	0.337

[a] $\bar{C}_p$ in units of cal/g-K.
[b] 22.80 mg sample.
[c] 49.14 mg sample.
[d] 53.58 mg sample.